Excitonic Photoluminescence in Semiconductor Quantum Wells: Plasma versus Excitons

S. Chatterjee, C. Ell, S. Mosor, G. Khitrova, and H. M. Gibbs
Optical Sciences Center, The University of Arizona, Tucson, Arizona 85721-0094, USA

W. Hoyer, M. Kira, and S. W. Koch
Department of Physics and Materials Sciences Center, Philipps-University Marburg, Renthof 5, 35032 Marburg, Germany

J. P. Prineas
Department of Physics and Astronomy, University of Iowa, Iowa City, Iowa 52242, USA

H. Stolz
Department of Physics, University of Rostock, Universitätsplatz 3, D-18051, Rostock, Germany
(Received 5 September 2003; published 13 February 2004)

Time-resolved photoluminescence spectra after nonresonant excitation show a distinct 1*s* resonance, independent of the existence of bound excitons. A microscopic analysis identifies exciton and electron-hole plasma contributions. For low temperatures and low densities, the excitonic emission is extremely sensitive to details of the electron-hole-pair population making it possible to identify even minute fractions of optically active excitons.

DOI: 10.1103/PhysRevLett.92.067402 PACS numbers: 78.67.De, 42.50.–p, 71.35.–y, 78.70.–g

Since an intrinsic semiconductor in thermal equilibrium at low temperature has a full valence band and an empty conduction band, any nonresonant excitation leads to a genuine nonequilibrium state with electrons in the conduction band and a corresponding number of holes in the valence band. Because of the attractive part of the Coulomb interaction, this electron-hole plasma can partly transform into Coulomb-bound pairs (excitons) under suitable conditions. Obviously, the knowledge of the specific form of the many-body state is of crucial importance when developing semiconductors with excitons toward and beyond regimes well known in atomic optics, such as Bose-Einstein condensation. For a long time, photoluminescence (PL) at the spectral position of the 1*s* exciton resonance has been considered as evidence for the existence of excitons. The rise of the 1*s* PL after nonresonant excitation of a semiconductor was interpreted as buildup of an exciton population [1–6], and the PL decay was used to describe exciton recombination [7,8]. However, recently a microscopic theory predicted that PL at the 1*s* resonance can also originate from a pure electron-hole plasma before any exciton formation has taken place [9]. Accordingly, PL at the spectral position of the 1*s* resonance would not prove the existence of excitons, and previous interpretations may be in question. Indeed, in nonresonantly excited time resolved PL measurements the 1*s* resonance is developed on a sub-ps time scale at 100 K [10], much faster than any expected exciton formation time.

Information about exciton formation can be gained by performing THz experiments [11]. However, currently the THz results are inconclusive. Kaindl *et al.* [12] observed the buildup of the induced absorption corresponding to the exciton 1*s* to 2*p* transition showing exciton populations with rather slow formation times of 100's of ps to ns. They claim to observe a nearly complete formation of excitons 1 ns after excitation, while Chari *et al.* [13] found only plasma contributions, i.e., no exciton populations. Also, THz absorption is sensitive to both dark and bright excitons, and cannot answer if and how exciton populations influence the PL. Here we address the following questions: Is the 1*s* PL ever dominated by plasma emission? If so, is it always dominated by plasma emission; i.e., what can we learn about exciton populations from the 1*s* PL and nonlinear absorption?

After ps continuum excitation, time resolved PL and corresponding probe absorption measurements are performed under identical conditions on a ns time scale. The sample (DBR42) consists of 20 molecular-beam epitaxy (MBE)-grown 8 nm $In_{0.06}Ga_{0.94}As$ quantum wells with 130 nm GaAs barriers; both sides are antireflection coated. This indium concentration places the 1*s* exciton resonance at 1.471 eV at 4 K, avoiding absorption in the bulk GaAs substrate that leads to impurity emission at 1.492 eV from unintentional carbon in the substrate. The results, checked on several other samples including a sample grown in a different MBE system, are insensitive to exciton linewidths or to interfacial or alloy disorder. Single-quantum-well data were noisier but exhibited a similar behavior, excluding significant radiative coupling effects. We excite nonresonantly 13.2 meV above the 1*s* resonance, into the heavy-hole continuum but below the light-hole resonance. The laser pulses are generated by a Ti:sapphire oscillator emitting 100 fs pulses at 80 MHz. Because of the long PL lifetimes, we use a pulse picker to reduce the repetition rate to 2 MHz and sweep slowly the

Hamamatsu streak camera, decreasing the PL time resolution to 90 ps. For spectrally selective excitation, a tunable 3 ps pulse is generated in a pulse shaper. The pump spot is focused to 60 μm diameter, 3 times larger than the probe spot. Both probe and PL are collected in transmission geometry and spectrally resolved with identical grating monochromators with a spectral resolution of 0.8 meV [14]. The probe transmission is detected with a liquid nitrogen cooled Si charge-coupled device. The carrier densities at different time delays are estimated from a calibration curve showing the peak height of the nonlinear absorption at 10 ps versus the initial carrier density.

Figure 1 displays measured PL spectra 1 ns after nonresonant excitation for three different densities (solid line). All PL spectra exhibit a distinct peak at the $1s$ exciton resonance (0 meV). The second peak 6.5 meV above is due to emission at the $2s$ resonance; the energetic separation of the resonances yields an 8 meV binding energy. The continuum PL exhibits an exponential falloff towards higher energies, from which a carrier temperature is extracted via the Boltzmann factor $\exp(-\Delta E/k_B T)$ by a least squares fit. In order to get a small standard deviation for the temperature values, it is necessary to detect several meV of continuum emission; this requires 4 to 5 orders of magnitude dynamic range.

Carrier temperatures extracted from the spectra in Fig. 1 are density dependent and vary from 13.5 K at the lowest density to 20.7 K at the highest density. Even at later times, they never reach the lattice value of 4 K [15–17]; the lowest temperature measured was 10.5 ± 0.5 K (2.8 ns after excitation for an initial carrier density of $n = 2.9\ \mu\text{m}^{-2}$). For a lattice temperature of 50 K, we find identical lattice and carrier temperatures after 0.1 ns.

To compare many spectra as a function of density and temperature, it is convenient to define a single parameter β to characterize each spectrum. In thermodynamic equilibrium, one expects the PL to be proportional to the absorption coefficient α times a Bose distribution function $g(\hbar\omega - \mu) = 1/(\exp^{(\hbar\omega-\mu)/k_B T} - 1)$, i.e., $I_{\text{PL}}^{\text{eq}}(\hbar\omega) \propto g(\hbar\omega - \mu)\alpha(\hbar\omega)$ where μ is the joint chemical potential of the electron-hole plasma; this is known as the Kubo-Martin-Schwinger (KMS) relation [18]. We then define $\beta = I_{\text{PL}}(1s)/I_{\text{PL}}^{\text{eq}}(1s)$ as in [17]. $I_{\text{PL}}^{\text{eq}}(\hbar\omega)$ is found by multiplying the measured nonlinear α by a Boltzmann factor to approximate the Bose function, using the temperature extracted from the measured continuum emission and normalizing it to agree with the measured continuum PL; see dashed lines in Fig. 1. Thus β quantifies how the $1s$ emission of a given spectrum differs from that expected from the measured absorption assuming validity of the KMS relation.

Figure 2 displays the density dependence of β for lattice temperatures of 50 K (top) and 4 K (bottom). We find significant deviation from $\beta = 1$ for all densities, temperatures, and times, implying that KMS is never valid for the configurations studied here. The 50 K result varies only slightly across the investigated density range. For the lower lattice temperature, we find pronounced deviations from the thermal equilibrium result particularly for low densities. For elevated densities, β exhibits an increase to values of around 0.5.

In order to analyze the experimental observations, we apply our microscopic theory that treats Coulomb interacting electrons and holes, phonons, and a quantized light field. The details of the theory can be found in previous

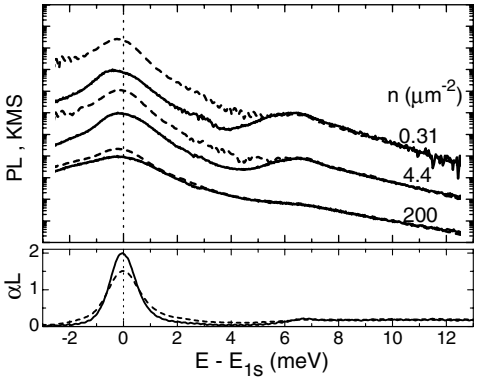

FIG. 1. Experimental PL spectra (solid lines) for a lattice temperature of 4 K are compared to the KMS result $I_{\text{PL}}^{\text{eq}}(\hbar\omega)$ (dashed lines), i.e., the measured nonlinear αL multiplied by the Boltzmann factor $\exp(-\Delta E/kT)$. PL is integrated from 0.95 to 1.05 ns after nonresonant excitation, and the densities are for $t = 1$ ns. The corresponding curve pairs are vertically offset by two decades. The bottom graph shows the nonlinear absorption spectra for the highest (dashed line) and lowest densities on a linear scale.

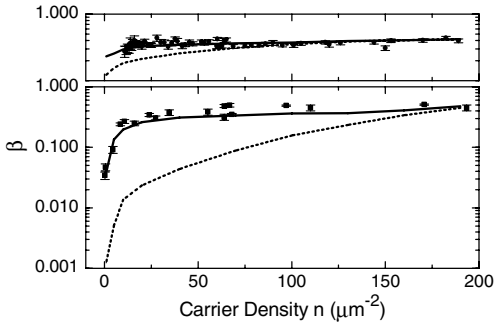

FIG. 2. β versus carrier density. Full squares refer to experimental values taken at 1 ns after nonresonant excitation at a lattice temperature of 4 K. The densities refer to densities at 1 ns. The theoretical values (dotted line) are calculated using the PL formula (1) for a pure electron-hole plasma with a carrier temperature of 16 ± 2 K. The solid line shows a theoretical fit including a $q = 0$ exciton contribution. Top: same for 50 K lattice temperature and extracted electron-hole plasma temperature of 50 ± 3 K; the theoretical curves are computed for a carrier temperature of 48 K.

publications [9,19]. This theory, evaluated at the level of a Hartree-Fock approximation first predicted luminescence at the exciton energy without exciton populations [9]. Meanwhile, we have extended the analysis to include also electron-hole correlations and bound excitons. We use an adiabatic treatment of the photon-assisted polarizations such that the steady-state luminescence can be obtained from

$$I_{\mathrm{PL}}(\omega) \propto \frac{|d_{cv}^2|\omega}{\varepsilon_{\mathrm{bg}}} \mathrm{Im}\Big[\sum_{\nu} \frac{\phi_\nu^r(r=0)}{E_\nu - \hbar\omega - i\gamma_\nu} \times \sum_{k,k'} [\phi_\nu^l(k)]^\star \langle a_{c,k'}^\dagger a_{c,k} a_{v,k'} a_{v,k}^\dagger \rangle \Big], \tag{1}$$

where $a_{\lambda,k}^\dagger$ creates an electron in band $\lambda = c, v$ in quantum state k. The prefactor in Eq. (1) is determined by the square of the dipole matrix element $|d_{cv}|^2$ and the background dielectric constant $\varepsilon_{\mathrm{bg}}$ [20]. Equation (1) is reminiscent of the famous Elliott formula for bandgap absorption [21]; it contains a sum over excitonic states, and the resonances of the denominator show that the PL peaks at the same excitonic energies as the absorption. In contrast to the absorption, however, the strength of the PL is not only determined by the exciton wave functions but also by the source term $\sum_{k,k'} (\phi_\nu^l(k))^\star \times \langle a_{c,k'}^\dagger a_{c,k} a_{v,k'} a_{v,k}^\dagger \rangle$. This source contains a plasma contribution $[\phi_\nu^r(r=0)]^\star \sum_k |\phi_\nu^l(k)|^2 f_k^e f_k^h$ which is always present as soon as electrons and holes are excited. Moreover, the source term can also describe incoherent bound exciton correlations which may or may not be in the system.

The theory-experiment comparison over the experimentally relevant density regime requires the proper description of the microscopic Coulomb scattering which is different for the correlation terms in comparison to the scattering of the photon-assisted polarizations. The exciton basis used in the calculations is not the usual low-density one; instead, left- and right-handed basis functions $\phi^{l/r}$ have to be taken into account. Furthermore, not only the eigenenergies $E_\nu(\omega)$ but also the broadenings $\gamma_\nu(\omega)$ depend on the excitonic index and the emission frequency. Separating the exciton and plasma populations, we evaluate our theory and determine β. The respective plasma distributions and exciton populations are treated as input to the theory, and a fit to the measured PL spectra is obtained by varying the optically active ($q = 0$) $1s$-exciton population. Thus, this formulation of the theory allows us to formally distinguish between electron-hole plasma and optically active bound excitons as different possible sources to excitonic PL.

Computed spectra are shown in Fig. 3: the pure plasma PL (dotted line) is compared to the KMS result (dashed line) obtained from the computed absorption. The corresponding β's are plotted as dotted lines in Fig. 2. At 50 K, the bare plasma emission shows good agreement with the experimental β's over almost the whole density range. Even for 4 K, the highest density results agree. Note that the exciton absorption is still very pronounced with the peak reduced by only 25%. This answers our first question: the $1s$ PL can be dominated by electron-hole plasma emission, and the spectra explained by a pure plasma theory; this is the case at high temperatures and even at low temperatures for higher densities.

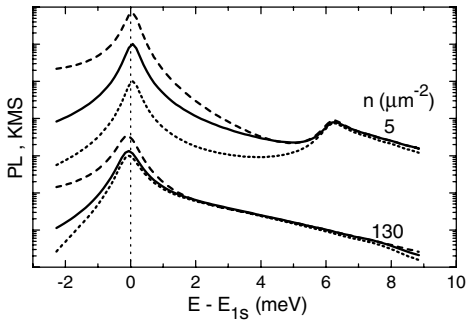

FIG. 3. Theoretical PL spectra for various densities for a carrier temperature of 16 K: pure plasma (dotted line) and including excitons (solid line). The exciton contributions used are chosen to give agreement with the experimental β as shown in Fig. 2. The KMS result (dashed line) is obtained by multiplying the computed nonlinear αL by the Boltzmann factor.

Figure 2 also shows that at 4 K and low to intermediate densities, the pure plasma calculation underestimates β. We attribute the stronger measured $1s$ emission to the presence of incoherent bound $1s$-exciton populations and test this hypothesis by adding optically active $q = 0$ excitons in the theory. Figure 3 shows that this addition strongly enhances the $1s$ PL. Since the plasma contribution changes quadratically with the carrier density, even minute exciton fractions result in a strong enhancement of the $1s$ resonance. The addition of excitons allows us to obtain an excellent theory-experiment agreement for β for all densities; see solid lines in Fig. 2.

Figure 4 shows the bright excitons necessary for that agreement. When the $1s$-exciton distribution is expressed as $N_X(q) = N_X(q=0)F(q)$ with $F(q=0) = 1$, only the

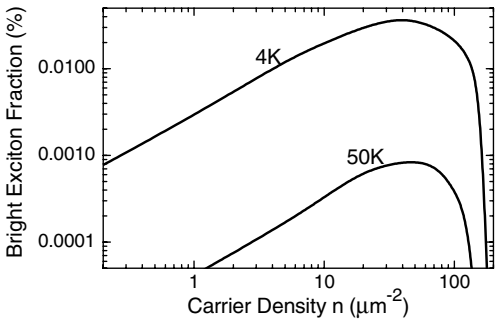

FIG. 4. Optically active $q = 0$ exciton contributions as a function of the carrier density.

$q = 0$ value can be deduced from the theory-experiment comparison. Thus, it is impossible to determine the total fraction of excitons from PL. However, the fraction of bright excitons can be estimated by using a constant distribution of excitons within the light cone. A maximum bright exciton fraction of less than 0.04% compared to the total amount of electrons and holes is found. If one wants to extract total bright and dark exciton fractions, additional assumptions on the center-of-mass distribution of the $1s$ excitons have to be made. If we assume a thermal distribution at 4 K, the largest value in Fig. 4 corresponds to a total exciton fraction of 4%. If significant hole burning [11,22] in the $1s$ distribution around $q = 0$ is present, this number could be much larger. This answers our second question: at low temperatures and for low and intermediate densities, the $1s$ PL is dominated by the recombination of excitons, even though the density of optically active excitons may be only a small fraction of the plasma density. Consequently, depending upon temperature and density, excitonic PL can be almost entirely from the plasma or almost entirely from excitons.

Even though our PL studies cannot determine the total exciton fraction or the detailed exciton distribution function, our results clearly show an increased importance of excitons at lower lattice temperatures and intermediate densities. This observation is in qualitative agreement with exciton formation studies in quantum wires [19]. Because of kinetic arguments, exciton formation after nonresonant excitation should be most efficient at intermediate densities. At low densities the probability for electron-hole collisions is too small, whereas at higher densities exciton binding is hampered by phase-space effects and screening of the attractive Coulomb interaction.

In conclusion, by carefully mapping out the parameter space of carrier density and lattice temperature, we have identified conditions under which the PL emission at the $1s$ resonance after nonresonant excitation into the continuum is dominated by the plasma or by an incoherent exciton population. We observe that the appearance of the $1s$-exciton resonance in PL is ubiquitous, independent of the existence of bound excitons and that the KMS relation is never fulfilled [23]. In particular, the $1s$ emission is always weaker than that predicted by KMS. Under suitable conditions excitons may form after nonresonant excitation, and we identify a regime of low temperature and intermediate density as most favorable.

The work is supported in Tucson by NSF (AMOP), AFOSR (DURINT), and COEDIP and in Marburg by the Deutsche Forschungsgemeinschaft through the Quantum Optics in Semiconductors Research Group, by the Humboldt Foundation and the Max-Planck Society through the Max-Planck Research prize, and by the Optodynamics Center of the Philipps-Universität Marburg.

[1] J. Kusano *et al.*, Phys. Rev. B **40**, 1685 (1989).
[2] T. C. Damen *et al.*, Phys. Rev. B **42**, 7434 (1990).
[3] R. Eccleston *et al.*, Phys. Rev. B **44**, 1395 (1991).
[4] P. W. M. Blom *et al.*, Phys. Rev. Lett. **71**, 3878 (1993).
[5] R. Kumar *et al.*, Phys. Rev. B **54**, 4891 (1996).
[6] M. Gulia *et al.*, Phys. Rev. B **55**, 16 049 (1997).
[7] J. Feldmann *et al.*, Phys. Rev. Lett. **59**, 2337 (1987).
[8] B. Deveaud *et al.*, Phys. Rev. Lett. **67**, 2355 (1991).
[9] M. Kira, F. Jahnke, and S. W. Koch, Phys. Rev. Lett. **81**, 3263 (1998).
[10] G. R. Hayes and B. Deveaud, Phys. Status Solidi A **190**, 637 (2002).
[11] M. Kira *et al.*, Phys. Rev. Lett. **87**, 176401 (2001).
[12] R. A. Kaindl *et al.*, Nature (London) **423**, 734 (2003).
[13] R. Chari *et al.*, in postdeadline papers of the Quantum Electronics and Laser Science Conference (unpublished), Paper No. QThPDA9.
[14] To better utilize the dynamic range of the streak camera a film neutral density filter was placed at the exit plane of the corresponding monochromator reducing the fluence by 40 for all energies <1.474 eV. The shown data are multiplied by this factor to present them undistorted.
[15] K. Leo *et al.*, Phys. Rev. B **37**, 7121 (1988).
[16] H. W. Yoon, D. R. Wake, and J. P. Wolfe, Phys. Rev. B **54**, 2763 (1996).
[17] R. F. Schnabel *et al.*, Phys. Rev. B **46**, 9873 (1992).
[18] R. Kubo, J. Phys. Soc. Jpn. **12**, 570 (1957); P. C. Martin and J. Schwinger, Phys. Rev. **115**, 1342 (1959).
[19] W. Hoyer, M. Kira, and S. W. Koch, Phys. Rev. B **67**, 155113 (2003).
[20] Our calculations are performed for finite quantum well widths and infinite barrier heights. We adjust the effective well width such that our calculations reproduce the experimentally measured exciton binding energy. $m_h/m_e = 3$ as determined using $k \times p$ theory, the other material parameters cancel out the β calculations.
[21] R. J. Elliott, Phys. Rev. **108**, 1384 (1957).
[22] C. Piermarocchi *et al.*, Phys. Rev. B **53**, 15 834 (1996).
[23] Because the experiment is pulsed, the carrier density decays with time. The temporal evolution of β followed over several ns shows that the decrease of β and the corresponding exciton fraction is fully parametrized by the density decay. Thus, β depends not upon past history, but only upon the momentary carrier density and temperature, as needed for comparison with a quasi-steady-state theory.